



# Severer nodular lesion in white matter than in gray matter in simian immunodeficiency virus-infected monkey, but not closely correlated with viral infection

Jingdong Zhang<sup>1,✉</sup>, Howard Fox<sup>2</sup>, Huangui Xiong<sup>2,✉</sup>

<sup>1</sup>Department of Anesthesiology, University of Cincinnati College of Medicine, Cincinnati, OH 45267, USA;

<sup>2</sup>Department of Pharmacology and Experiment Neuroscience, University of Nebraska Medical Center, Omaha, NE 68198, USA.

## Abstract

Immune cell accumulation and white matter anomaly are common features of HIV (human immunodeficiency virus) -infected patients in combination antiretroviral therapy (cART) era. Neuroimaging tests on cART treated patients displayed prominent diffuse white matter lesions. Notably, immune cell nodular lesion (NL) was a conspicuous type of pathological change in HIV/SIV (simian immunodeficiency virus) infected brain before cART. Therefore, we used SIV infected brain to investigate the distribution of those NLs in gray and white matters. We found a significant higher number of NLs in white matter than that in gray matter. However, virus infection correlated with macrophage NLs but not with microglia NLs, especially in white matter. In addition, NLs interrupted white matter integrity more severely, since even tiny nodules could disconnect nerve fibers in white matter tracts. In the gray matter with dense myelinated axons, NLs obviously encroached those fibers; in the area of few myelinated axons, small nodules well co-localized with extracellular matrix between neurons.

**Keywords:** simian immunodeficiency virus-infected monkey, white matter tract, nodular lesions, microglia nodules, perivascular cuffing, nerve fiber disconnection

## Introduction

Introduction of combinational antiretroviral therapy (cART) has resulted in a significant reduction in the prevalence of human immunodeficiency virus type 1 associated encephalitis (HIVE) and associated dementia (HAD). While remarked poliodystrophy has changed to focal (burnt-out type) or diffuse white matter anomalies, HAD has shifted to mild or

moderate neurological disorders<sup>[1-2]</sup>. Although the mechanism of brain gray or white matter lesions in cART era may be different from previous HIVE due to cocktail antiretroviral treatment, monocyte infiltration and microglia activation are still the common entities<sup>[3-4]</sup>. Nodular lesion, characterized by cell clusters of different sizes formed by immune cells, was a type of pathological change frequently observed in HIVE or simian immunodeficiency virus

✉Corresponding authors: Jingdong Zhang, Department of Anesthesiology, University of Cincinnati College of Medicine, 231 Albert Sabin Way, Cincinnati, OH 45267, USA. Tel: +1-513-558-2472, E-mail: [zhang2jd@ucmail.uc.edu](mailto:zhang2jd@ucmail.uc.edu); Huangui Xiong, Department of Pharmacology and Experiment Neuroscience, University of Nebraska Medical Center, Omaha, NE 68198, USA. Tel: +1-402-559-5140, E-mail: [hxiang@unmc.edu](mailto:hxiang@unmc.edu).

Received 11 May 2018, Revised 16 April 2019, Accepted 04 June

2019, Epub 28 August 2019

CLC number: R512.91, Document code: A

The authors reported no conflict of interests.

This is an open access article under the Creative Commons Attribution (CC BY 4.0) license, which permits others to distribute, remix, adapt and build upon this work, for commercial use, provided the original work is properly cited.

encephalitis (SIVE) brain<sup>[5-7]</sup>. While large size nodular lesions in cART treatment that usually concomitant with opportunistic infection<sup>[7-8]</sup> have been generally eliminated, it is not clear whether or not small nodular lesions are still prevalent, although loosely aggregated microglia had been encountered in postmortem sample of a cART case<sup>[9]</sup>. Neuroimaging studies of cART treated acquired immunodeficiency syndrome (AIDS) patients showed white matter linear structure disruption, reflected by fractional anisotropy declination and mean diffusivity increment<sup>[10-11]</sup>. Meanwhile, a frequently-observed HIV-1 related brain pathology in cART era is focal burnt-out white matter anomalies<sup>[1-2]</sup>. Thus, whether those burnt-out white matter impairment and/or white matter linear interruptions detected by neuroimaging exam have resulted from small-size nodular lesions remains unclear. There is also no literature report to indicate the correlation between aforementioned neuroimaging and neuropathological findings.

Notably, in early postmortem studies of patients with HIVE, investigators had observed that white matter damage was recurrently associated with macrophage/microglia nodules and multinucleate giant cells, which is a hallmark of pathological change<sup>[5-7]</sup>. In studies using a neurovirulent strain of SIV to infect monkeys without any opportunistic infection, numerous nodular lesions in white matter were also observed<sup>[12-13]</sup>. However, previous studies did not explicitly enumerate the nodules, classify types of nodules and analyze their distribution morphometrically in gray and white matters in either HIVE or SIVE brain<sup>[7-8, 12-13]</sup>. Clarifying the preferential distribution of nodular lesions in gray or white matter may provide some clues for detecting a possible pathogenic source of focal burnt-out white matter damage in brains of AIDS patients receiving cART treatment. Further, this distribution may also reflect the potential target of monocyte carrying antiretroviral nanomedicine<sup>[14-15]</sup>. In addition, whether these cellular clusters are formed predominantly by HIV/SIV-infected immune cells such as infected microglia or macrophages, or primarily by non-infected immune cells, is an unavoidable topic.

Therefore, in the present study, we used ionized calcium-binding adapter molecule 1 (Iba-1) immunofluorescence staining to label microglia and macrophages<sup>[16-17]</sup> in a small cohort SIVE brain. We divided nodular lesions herein into microglia nodule (MN) and perivascular macrophage nodule that had been termed as perivascular cuffing (PC)<sup>[18]</sup>, and formation of MN and PC may be underlined by

different mechanism<sup>[18-19]</sup>. We applied SIV Nef p27 to identify cells which were infected by SIV and undergoing virus replication, because p27 is an indicator of early infection and viral replication<sup>[20-22]</sup>. In addition, myelin basic protein (MBP) and neurofilament (NF) immunostaining combined with Iba-1 labeling was carried out to disclose whether and how the nodular lesions would injure gray and/or white matter, to evaluate and compare the degree of these lesions in gray and white matters.

## Materials and methods

### SIV-infected monkeys and brain sample resource

The protocol was carried out in accordance with the National Institutes of Health "Guide for the Care of Laboratory Animals in Research" and approved by the Institutional Animal Care and Use Committee of The Scripps Research Institute at La Jolla, California. Based on the previous report by Dr. Howard Fox<sup>[23]</sup>, all animals were SIV, SRV-type D and *Cercopithecine herpesvirus 1* virus negative before SIV inoculation. A total of 12 Indian rhesus macaques (*Macaca mulatta*), the animals used in previous publications<sup>[23]</sup> were the experimental subjects. The animals were inoculated intravenously with approximately 10<sup>4</sup> PFU (plaque forming units) of SIVmac251 virus and were sacrificed 66 to 208 days after inoculation. The major reasons for earlier euthanasia were diarrhea without appetite and pneumonia with hard respiration. The neurological symptoms were summarized in that early publication<sup>[23]</sup>. Plasma viremia before necropsy was varied from 10<sup>6</sup> to 10<sup>8</sup> copies/mL. The frontal, parietal and occipital brains, from 4 healthy and 8 SIV-infected monkeys, were embedded into paraffin blocks and were used in the present study.

### Immunofluorescent staining and evaluation of nodular lesions

The monkey's brain blocks were cut into 7- $\mu$ m in thickness. Deparaffinization, rehydration and antigen unmasking were combined to a single step by using Declare/Trilogy (Cell Marque, USA) in pressure cooker for 15 minutes. After blocking non-specific antigens, rabbit anti-Iba-1 (1:250, Wako Chemicals USA Inc., USA) was applied to label microglia and macrophages. Mouse anti-SIV Nef protein (p27, 1:500, Santa Cruz Biotechnology, USA) in combination of anti-Iba-1 was applied to examine SIV-infected microglia and macrophages. Rat anti-myelin basic protein (MBP, 1:200, Millipore, USA), or mouse anti-human neurofilament-70 (NF, clone

2F11; 1:200, Dako, USA), combined with rabbit anti-Iba-1 was used to evaluate injuries of either myelinated or unmyelinated nerve fibers by nodular lesions. Either Alexa Flour 488 or 594 conjugated secondary antibodies (1:200, Molecular Probes, USA) was used to visualize the primary labeling. Control immunofluorescent staining was performed without using primary antibodies but after blocking procedure.

### Enumeration of MN and PC

Enumeration of MN and PC was performed in frontal brains of eight SIV-infected monkeys. The labeled MN and PC in the 0.3 cm thick (distributed in about 420–430 sections at 7  $\mu\text{m}$  in thickness) block from each monkey's frontal brain were counted by using stereological software (Stereo-Investigator v 9.14, MBF Bioscience, USA). As the diameters of MN and PC are generally  $\geq 100 \mu\text{m}$  and they allocate across about 14 (100  $\mu\text{m}/7 \mu\text{m}$ ) consecutive sections, every-14<sup>th</sup>-section was counted under microscope (**Fig. 1A**). As the block thickness was about 0.3 cm (**Fig. 1B**), altogether about 30 sections (30 $\times$ 14=420) from each monkey's brain were enumerated. Then, the area of gray and white matter on each section was measured under an anatomic microscope by using a caliper. These areas ( $\text{cm}^2$ ) multiplying the block thickness 0.3 cm (**Fig. 1B**) gave rise to a whole volume of the frontal gray or white matters by cubit

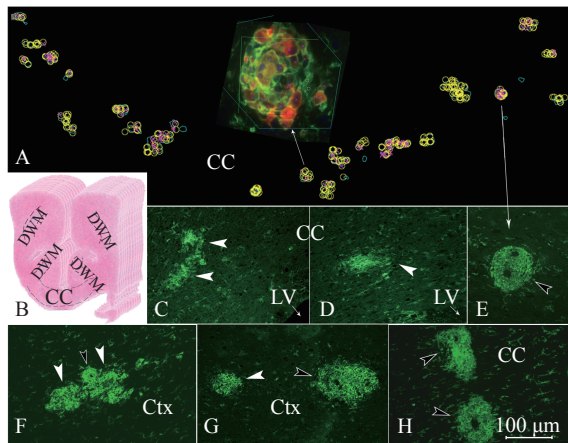


**Fig. 1** Distribution of MNs and PCs in frontal CC and Ctx. A: Programmed image by Stereo-Investigator in which all of Iba-1 labeled cell clusters  $\geq 100 \mu\text{m}$  were circled and counted. MNs and PCs were manually marked after scanning of each slide. The inset (pointed by an upward arrow) shows a programmed gridded area by software, in which Iba-1 (green), SIV p27 (red) and double labeled cells were counted, respectively. B: A reconstructed frontal brain block (about 0.3 cm in thickness) by HE stained sections. C–E and H: Representative microimages showing different morphology of MNs (arrowheads) and PCs (opened arrowheads) in frontal CC. F and G: The MNs and PCs located in frontal Ctx. MNs: microglia nodules; PCs: perivascular cuffs; DWMT: deep white matter; LV: lateral ventricle; Ctx: cortex; CC: corpus callosum.

cm ( $\text{cm}^3$ ). Final density of MN and PC in each frontal brain was summarized as the number of MN/ $\text{cm}^3$  and PC/ $\text{cm}^3$ .

### Enumeration of p27 positive cells within MNs and PCs in gray and white matters

The software could recognize the color such as red, green and yellow, but could not distinguish the MN or PC. Thus, it is necessary to set up the software to remember red and yellow at first and can remember their locations under 10 $\times$  lens. When the objective lens was shifted to 40 $\times$  to recognize the individual colored cells, the software guided the 40 $\times$  lens automatically to recorded coordinates. In these positions or nodules, under the 40 $\times$  lens, we clicked the mouse to mark red or green or yellow cells (**Fig. 1A**), and then the number of these "marks" would be automatically read and saved through a computer. However, the operator had to distinguish a nodule as either MN or PC manually and recorded the number respectively. The total red+green and single green cells were recorded as SIV infected and none infected cells per 30 sections, because the counting was performed in 30 sections evenly through the whole front brain.

### Statistical analysis

Paired *t*-test comparison was used for analysis of the number of the MN and PC per cubic centimeter between gray and white matter tissues from each SIV-infected monkeys, plotted in **Fig. 2A**. One-way ANOVA with Newman-Keuls Multiple Comparison Posttest of each column was applied to analyze distribution of p27 within MNs and PCs in gray and white matters, plotted into **Fig. 2C**. Statistics were performed and plotted using Graph Pad Prism 5 (GraphPad Software Inc., USA) and significance was indicated as "\*" for  $P < 0.05$ , "\*\*\*" for  $P < 0.01$  and "\*\*\*\*" for  $P < 0.001$ .

## Results

### Distribution of MNs and PCs in gray and white matters of SIV-infected monkeys

#### *Distribution of MNs in investigated frontal gray and white matters*

Clusters of cells labeled with Iba-1 in parenchyma and perivascular regions were observed in frontal brain of all eight SIV-infected monkeys (**Table 1, Fig. 1**). As both microglia and macrophage express Iba-1, the MN might represent microgliosis (**Fig. 1C, D, F and G**) and the PC were probably infiltrated monocytes and derived macrophages (**Fig. 1E–H**). In

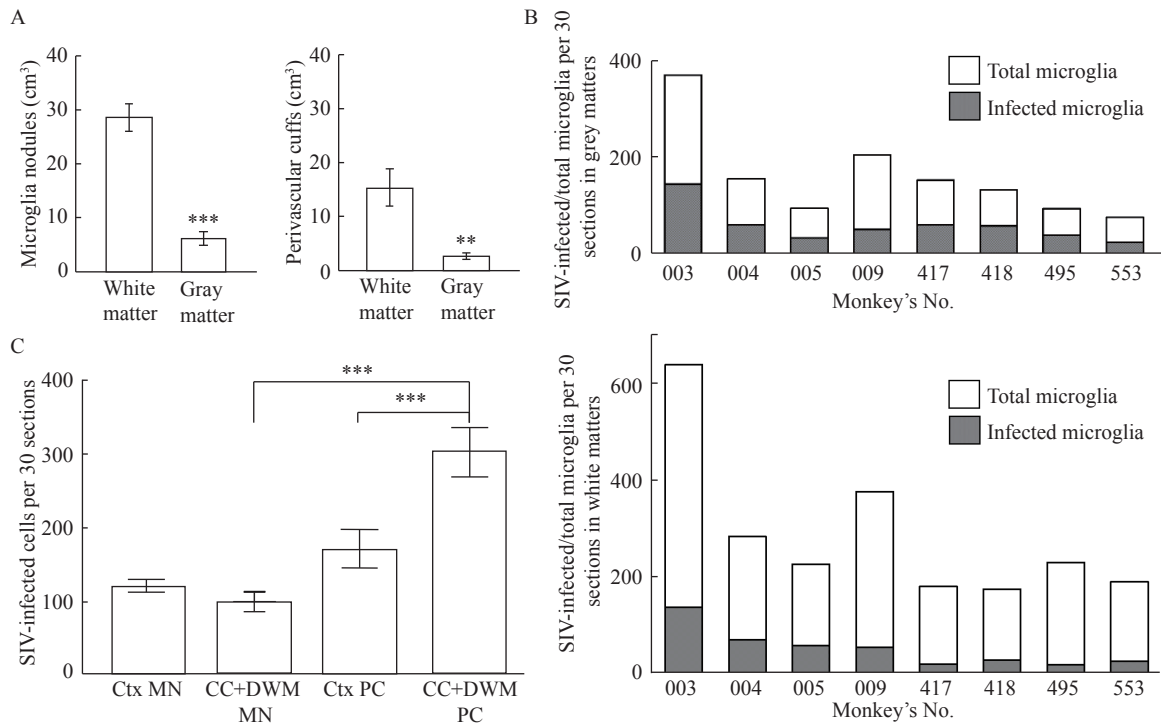


**Fig. 2 Comparison of numbers of MNs, PCs and infected cells in those MNs and PCs, in gray and white matters.** A: The number of MNs and PCs per cm<sup>3</sup> summarized from *Table 1*, from 8 SIV-infected front brain (represented by *Fig. 1B*). Both MN and PC numbers in white matter is highly significantly more than that in gray matter. B: The ratio of infected to uninfected microglia in MNs in gray and white matters of each monkey. C: Statistical summary of distribution of SIV-infected cells among MNs and PCs in gray and white matters. Infected PC macrophages are highly significantly more than infected MN microglia in the white matter. Meanwhile, infected macrophages are highly significant prevalent in white matter PCs than that in gray matter PCs. \*\**P*<0.01, \*\*\**P*<0.001. MNs: microglia nodules; PCs:perivascular cuffings; CC: corpus callosum; Ctx: cortex; DWM: deep white matter.

gray matter, the MNs were scattered in frontal cortex (Ctx) (*Fig. 1F* and *G*) with more MNs located near by the cortex surface or by border of gray and white matter. In white matter, these MNs were observed in the whole frontal corpus callosum (CC), a large white matter tract linking bilateral hemispheres, and in deep white matter bridging between lobes and gyri<sup>[24]</sup> (*Fig. 1*). We judged whether they are MN or PC by looking for a blood vessel cavity inside of the cell cluster and we identified the nodule as PC if a central or eccentric cavity was regarded. The number of MNs in gray and white matters of each SIV-infected monkey (*Table 1*) was statistically compared and the number of MNs in frontal white matter was significantly higher than that in frontal cortex (*Fig. 2A*).

*Distribution of PCs in investigated frontal gray and white matters*

The characteristic of the PC is that small vasculature structure was generally visualized and layers of Iba-1 labeled cells surrounded the hollow of blood vessel (*Fig. 1E–H*). Sometimes, MN and PC were intermingled with each other (*Fig. 1F*). However, some PCs around brain capillaries might be mistaken as MNs if the cavity is compressed to close by aggregated cells (*Fig. 1F*). In this case, overlapped circled cellular layers observed under higher magnification lens is a criterion to distinguish PC from MN. Evidently, more PCs were in white matter than in gray matter (*Table 1*). Statistic comparison of

Monkey's No.	003	004	005	009	417	418	495	553
MN in white matter	39	20	35	27	20	31	24	34
MN in gray matter	13	0.5	10	7	3	8	3	4
PC in white matter	15	11	5	3	20	12	5	1
PC in gray matter	4	1	1	2	3	1	1	1

MN: microglia nodule; PC: perivascular cuffing; SIV: simian immunodeficiency virus.

the values showed the number of PCs in white matter was significantly higher than that in gray matter (**Fig. 2A**).

### Distribution of p27 in gray and white matter of SIV-infected monkeys

#### *Distribution of p27 positive cells in MNs on 30 observed sections*

Nef p27 is synthesized at an early stage of infection and can enhance infectivity of the newly assembled viral particles during viral replication<sup>[20–21]</sup>. More importantly, Nef p27 represents neurovirulence of the virus in SIV infection, and a full-size p27 is crucial for viral replication and diffusion in the monkey's brains<sup>[21–22]</sup>. Thus, we used p27 to label infected microglia. A representative counting window is shown in **Fig. 1A** inset. The ratio of infected to uninfected microglia in gray and white matter of each monkey is shown in **Fig. 2B**. Then, we statistically compared the number of SIV infected microglia in the gray and white matter MNs, and found no significant difference (**Fig. 2C**). As we have noticed, p27 positive cells, namely infected microglia, in many white matter MNs were few (**Fig. 3A** and **B**) or even absent (**Fig. 4D**).

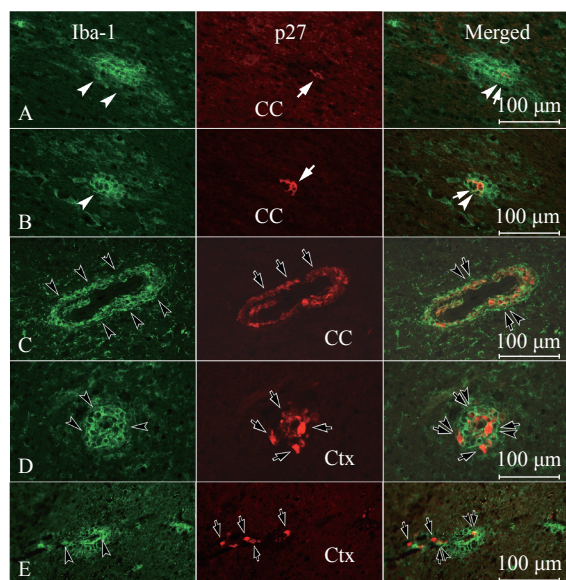


**Fig. 3** Distribution of p27 positive cells in MNs and PCs in CC, DWM and Ctx. A and B: Show low ratio of p27 labeled cells (arrows) among MN microglia (arrowheads) in the CC. C: Whereas, there are a large percentage of p27 positive cells (opened arrows) among macrophages in the PCs (opened arrowheads). D: Similarly in the Ctx, a large ratio of p27 labeled macrophages are situated in the PCs. While, a p27 single labeled cell is also seen, pointed by an opened arrow in "Merged" panel. E: p27 single labeled cells (opened arrows at "Merged" panel), and p27-Iba-1 double labeled macrophages (opened arrow and arrowheads) nearby a small PC in Ctx. CC: corpus callosum; Ctx: cortex.

As shown in **Fig. 4D** that was montaged figure from a serial of 10× microimages, only 3 among 12 MNs in that CC contained p27 labeled cells (arrows). Interestingly, some infected cells preferred to surround a MN than to situate inside of the MN (**Fig. 4C**).

#### *Distribution of p27 positive cells in PCs through 30 representative sections*

Whereas, Iba-1 positive cells in PCs of both gray and white matters were constantly co-labeled with p27. Thus, the number of p27-Iba-1 co-labeled cells, representing SIV infected macrophages, in the white matter was significantly higher than that in gray matter (**Fig. 2C**; **Fig. 3C** and **D**). In parallel, in the white matter, infected PC macrophages were significantly more than infected MN microglia (**Fig. 2C**,  $P < 0.001$ ). In addition, more or less p27 single labeled cells around PC (**Fig. 3D** and **E**) and/or MN (**Fig. 4C**) were visualized in both gray and white

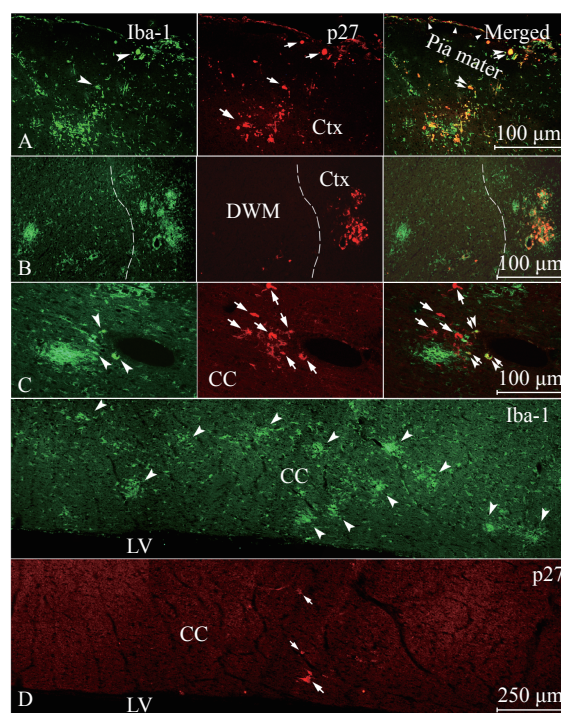


**Fig. 4** Preferential locations of SIV-infected cells in gray and white matters. A: In addition to preferential distribution of MNs in surface areas of the cortex, many SIV-infected cells (arrows) were observed along cortex surface under or close to pia mater. B: More p27 positive cells are encountered in the MNs located in the border area between the DWM or CC and Ctx. C: p27 labeled cells are also preferentially scattered around brain blood vessels in gray and white matter (indicated by arrows alone in "Merged" panel). D: A montaged image showing a large percentage of MNs in this CC do not harbor infected microglia at all. Meanwhile, more SIV infected cells (arrows) are distributed along border area close to ventricles. CC: corpus callosum; Ctx: cortex; DWM: deep white matter.

matters. It is not clear what cells are those Iba-1 negative infected cells, but some of them might be lymphocytes since infiltration of HIV-1 infected lymphocytes into the brain in AIDS cases had been reported previously<sup>[25]</sup>.

#### *Preferential locations of p27 positive cells among the MNs*

In the gray matter, it seemed that more infected cells were distributed in areas close to superficial pia mater (**Fig. 4A**), ventricle ependyma and border between gray and white matter (**Fig. 4B**). In the white matter, it appeared that SIV infected cells preferred to situate nearby or surround the blood vessels (**Fig. 4C**), or distributed close to the ventricles (**Fig. 4D**). In summary, the number of SIV infected cells correlated with the number of PCs in both gray and white matters. However, the number of infected microglia varied greatly in MNs and was not correlated with the number of MNs, especially in the white matter (**Fig. 4D**).

#### **Evidence of white matter tract disconnected by nodular lesions**

MBP is a major structural protein in the myelin sheath<sup>[26]</sup> and disruption of the MBP positive linear structure reflects the injury of myelin sheath, then myelinated nerve fibers. NF is an essential structural protein of myelinated and unmyelinated fibers<sup>[27]</sup>; disconnection of NF positive linear structure indicates the broken-down of the nerve fibers. We indeed observed an abundance of intruded injuries by nodular lesions on myelin sheath or nerve fibers by Iba-1 and MBP or NF double immunostaining (**Fig. 5**).

#### *An interesting phenomenon in cortex*

In the frontal cortex, heavier MBP labeling was observed in the upper layer IV (internal granular layer) and layer V (pyramidal layer). In contrast, no apparent MBP staining was seen in layers I–III (**Fig. 5A** and **B**). **Fig. 5A** shows a MN (arrowhead) located in cortical upper layer IV where the MBP stain is heavier, a MBP negative cavity is seen over there (small arrows). However, a MN found in layers II and III where there is no evident MBP labeling does not crop a cavity (**Fig. 5B**). This phenomenon suggests MN microglia might be electively encroaching myelin compound during formation of the MNs.

#### *Space-occupying nodular lesions cut nerve fibers*

Both MNs (arrowhead) and PCs (opened arrowheads) could damage the surrounding myelin sheaths and/or nerve fibers of either myelinated or

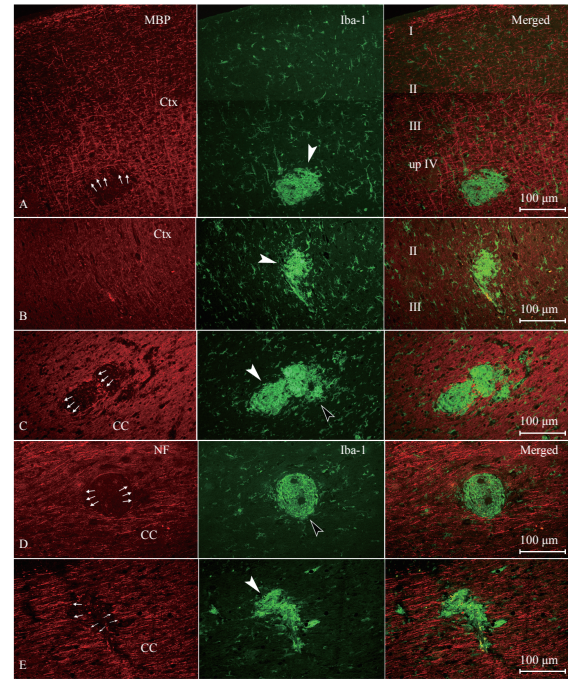


**Fig. 5** Detection of nerve fibers broken by nodular lesions using MBP or NF and Iba-1 double labeling. A: A MBP negative cavity (small arrows) is shown co-localized with a MN (arrowhead) in upper layer IV of the cortex, where the MBP immunoreactivity is heavier. B: But in layer II and III of the cortex where there is light MBP labeling, no such cavity is visualized when a MN is situated therein. C: There are dense myelinated fiber bundles in this part of the CC with heavy MBP immunoreactivity; therefore, MBP and Iba-1 double immunostain displayed clear MBP negative cavities (small arrows) herein. D and E: Consistently, NF and Iba-1 double labeling shows PCs (opened arrowhead) and MNs (arrowhead) broke NF positive nerve fibers (small arrows) those may either myelinated or unmyelinated in the CC. MBP: myelin basic protein; NF: neurofilament-70; CC: corpus callosum; Ctx: cortex.

unmyelinated. **Fig. 5C** shows a large nodule lesion composed of both MN and PC has encroached adjacent MBP positive myelin sheaths (small arrows) in the CC. Meanwhile, both MNs (arrowhead) and PCs (opened arrowhead) cut off NF positive nerve fibers (**Fig. 5D** and **E**) in the CC. These nerve fibers could be either myelinated or unmyelinated axon bundles.

## **Discussion**

As aforementioned, by searching PubMed, we did not see any report that precisely records the number of nodular lesions in gray and white matters in HIVE brain and comparison of their distributive preference. This is probably due to limited availability of an entire lobe of human brain with both gray and white matters. We have resolved this problem by using representative frontal brain of eight SIV-infected monkeys, and we divided these nodular lesions into

the MN and PC to enumerate them. Then, we demonstrated that the number of both MNs and PCs are significantly higher in white matter than that in gray matter. Meanwhile, cellular composition of the MNs and PCs are commonly different, which suggests formations of the MNs and PCs may undertake different mechanism. PCs in both gray and white matters might contain some microglia, but the majority of Iba-1 labeled PC clusters therein would be composed of infiltrated monocytes and their derived macrophages<sup>[18]</sup>. In circumstance of HIV-1 and SIV infection, virus infected monocytes infiltrate into the CNS and carry the virus in, which is termed as "Trojan horse" mechanism<sup>[18,28]</sup>. These infiltrated cells, either HIV-1/SIV infected or non-infected, could build up PCs quickly after initial system infection during acute HIV-1 or SIV infection stage<sup>[18]</sup>. This was confirmed by a case of iatrogenic HIV-1 infection patient who died 15 days after accidentally inoculation of the virus<sup>[29]</sup>. Postmortem study showed that obvious perivascular monocyte/macrophage cuffing had already formed in the brain of this patient<sup>[29]</sup>. This phenomenon suggests that the majority of PCs which we observed and counted might be formed in the early stage of SIV infection. Hence, according to our finding of highly significant numerous PCs distributing in white matter, it seems that white matter could recruit more monocyte/macrophage than could gray matter do during SIV or/and HIV-1 infection.

Coincidentally, a study in mice showed white matter CC expresses dramatically higher level mRNA of monocyte chemotactic protein-1, also classified as beta chemokine CCL2, than does cortex gray matter<sup>[30]</sup>. As we know, the CCL2 is a chemokine principally chemotactic for monocyte lineage populations<sup>[31]</sup>. Further in humans, in a postmortem study of MS cases, the authors found that chemokine CCL2 level in hippocampal white matter was significantly higher than that in gray matter<sup>[32]</sup>. These facts suggest white matter may exist higher chemotactic capability for monocytes than gray matter does. This could be a potential cause for higher number of PCs in white matter than in gray matter, especially at the early stage of the infection<sup>[29]</sup>. However, how to interpret conspicuous significantly higher number of MNs, assembled by brain resident microglia, observed in the white matter is still no direct clue. Monkeys used in this study had no any opportunistic infection that was considered as a pathogenic source of microglial nodular encephalitis in humans<sup>[8,33]</sup>. Thus, SIV infection or viral replication is the first element for us to consider for activation and aggregation of the microglia<sup>[19,34]</sup>. We performed SIV

Nef p27 immunostaining to analyze distribution of infected cells in gray and white matters and expected to see more SIV infected microglia in the white matter, which would parallel with higher number of MNs in the white matter. Paradoxically, the total number of SIV infected microglia in white matter is somewhat less than that in gray matter, with no much difference. This indicated that states of SIV infection do not parallel with aggregation of microglia and/or formation of the MNs. On the other hand, in line with the idea that white matter may have higher chemotactic capability for monocyte lineage, SIV infected monocytes/macrophages within PCs are significantly abundant than infected microglia in the white matter. Nonetheless, microglia might need being activated before they aggregated into nodules<sup>[13]</sup>. Pro-inflammation cytokines secreted by microglia would amplify the effect of viral infection through just a few infected microglia. Besides, infected perivascular macrophages secrete pro-inflammation cytokines that could either activate microglia. In addition, extracellular soluble viral proteins, such as HIV-1 Tat and gp-120, could probably elicit microglia activation<sup>[35-36]</sup>.

Pathologically, in order to determine whether these aggregated microglia or/and macrophages generate any kind of lesion *in situ*, we performed double labeling of Iba-1 and MBP or NF to examine the relationship between MNs/PCs and myelinated or unmyelinated nerve fibers. We observed that MNs and PCs overlapped with MBP negative cavities, which might be resulted from engulfing of sick myelin that exposed eat-me signal in the CC and deep white matter<sup>[37]</sup>. We also observed that MNs and PCs pushed away or interrupted the NF positive fibers surrounding the nodules and these injured fibers were possibly either myelinated or unmyelinated. We further disclosed an interesting phenomenon that the MNs or PCs might encroach myelinated nerve fibers even in gray matter. In the frontal cortex, pyramidal cells and other kinds of neurons mostly situate in layers II, III and upper layer IV; whereas, myelinated axons from pyramidal cells concentrated in deep layer IV, layer V and upper layer IV<sup>[24]</sup>. The MBP negative cavities were clearly observed to overlap with MNs or PCs in deep layer IV, layer V and upper layer IV. However, in the layers II and III where lacks of myelinated fibers, no cavity was visualized to overlay with MNs or PCs which seemed to be immersed in the extracellular matrix. Thus, we showed the evidence of MNs and PCs disconnecting the nerve fibers of either myelinated or unmyelinated in the current study. Of note, our previous observation on postmortem

immunostaining on the brain of a cART case unveiled existing of microglia clusters that was not as compact as those MNs observed in HIVE or SIVE cases<sup>[9]</sup>.

Clinically, regular cART seems to be not able to completely prevent infected monocyte infiltration and results in microglia activation and aggregation. However, as aforementioned, HIV/SIV enters the brain by a "Trojan horse" mechanism<sup>[18,28]</sup>. Could circulating monocytes haul any antiretroviral drug into the brain if they can carry the virus to perivascular spaces? Delivery of nanoparticles containing antiretroviral medicine into the brain by monocytes has been considered and studied in recent years<sup>[14–15]</sup>. The observations in the current work suggest the earlier application of nanoparticle carried antiretroviral medicine is possibly more beneficial for controlling nodular lesions in the white matter. Consequently, the related mild cognitive impairment and neurological soft signs may be better improved<sup>[38]</sup>. As we have known, the white matter tracts in CC and deep white matter conducts communication between two hemispheres and among global lobes and gyri<sup>[24]</sup> as cables carry signals between process-units. Miscommunication would happen if any part of the cables were disconnected or compressed, which may somehow lead to cognitive problem if it occurs in human brains.

### Acknowledgments

We warmly thank Ms. Rebecca Wilshusen for her direction and assistance in using Stereo-Investigator v 9.14 software and cell counting procedure, and appreciate Dr. Lee Mosley for his direction on organizing the imaging data. This study was supported by R01 NS063878, R01 NS077873 and P30 MH062261 (to H.X. and H.S.F.).

### References

- [1] Gray F, Chrétien F, Vallat-Decouvelaere AV, et al. The changing pattern of HIV neuropathology in the HAART era[J]. *J Neuropathol Exp Neurol*, 2003, 62(5): 429–440.
- [2] Everall IP, Hansen LA, Masliah E. The shifting patterns of HIV encephalitis neuropathology[J]. *Neurotox Res*, 2005, 8(1–2): 51–61.
- [3] Garvey LJ, Pavese N, Politis M, et al. Increased microglia activation in neurologically asymptomatic HIV-infected patients receiving effective ART[J]. *AIDS*, 2014, 28(1): 67–72.
- [4] Tavazzi E, Morrison D, Sullivan P, et al. Brain inflammation is a common feature of HIV-infected patients without HIV encephalitis or productive brain infection[J]. *Curr HIV Res*, 2014, 12(2): 97–110.
- [5] Navia BA, Cho ES, Petito CK, et al. The AIDS dementia complex: II. Neuropathology[J]. *Ann Neurol*, 1986, 19(6): 525–535.
- [6] Petito CK, Cho ES, Lemann W, et al. Neuropathology of acquired immunodeficiency syndrome (AIDS): an autopsy review[J]. *J Neuropathol Exp Neurol*, 1986, 45(6): 635–646.
- [7] Bell JE. The neuropathology of adult HIV infection[J]. *Rev Neurol (Paris)*, 1998, 154(12): 816–829.
- [8] Nebuloni M, Pellegrinelli A, Ferri A, et al. Etiology of microglial nodules in brains of patients with acquired immunodeficiency syndrome[J]. *J Neurovirol*, 2000, 6(1): 46–50.
- [9] Yang XL, Zhang JD, Duan L, et al. Microglia activation mediated by toll-like receptor-4 impairs brain white matter tracts in rats[J]. *J Biomedical Res*, 2018, 32(2): 136–144.
- [10] Wu Y, Storey P, Cohen BA, et al. Diffusion alterations in corpus callosum of patients with HIV[J]. *AJNR Am J Neuroradiol*, 2006, 27(3): 656–660.
- [11] Chen YS, An HY, Zhu HT, et al. White matter abnormalities revealed by diffusion tensor imaging in non-demented and demented HIV+ patients[J]. *NeuroImage*, 2009, 47(4): 1154–1162.
- [12] Xing HQ, Moritoyo T, Mori K, et al. Simian immunodeficiency virus encephalitis in the white matter and degeneration of the cerebral cortex occur independently in simian immunodeficiency virus-infected monkey[J]. *J Neurovirol*, 2003, 9(4): 508–518.
- [13] Xing HQ, Moritoyo T, Mori K, et al. Expression of proinflammatory cytokines and its relationship with virus infection in the brain of macaques inoculated with macrophage-tropic simian immunodeficiency virus[J]. *Neuropathology*, 2009, 29(1): 13–19.
- [14] Thomas MB, Gnanadhas DP, Dash PK, et al. Modulating cellular autophagy for controlled antiretroviral drug release[J]. *Nanomedicine (Lond)*, 2018, 13(17): 2139–2154.
- [15] Herskovitz J, Gendelman HE. HIV and the macrophage: from cell reservoirs to drug delivery to viral eradication[J]. *J Neuroimmune Pharmacol*, 2019, 14(1): 52–67.
- [16] Imai Y, Iyata I, Ito D, et al. A novel gene *Iba-1* in the major histocompatibility complex class III region encoding an EF hand protein expressed in a monocytic lineage[J]. *Biochem Biophys Res Commun*, 1996, 224(3): 855–862.
- [17] Ito D, Imai Y, Ohsawa K, et al. Microglia-specific localisation of a novel calcium binding protein, Iba-1[J]. *Brain Res Mol Brain Res*, 1998, 57(1): 1–9.
- [18] Kim WK, Corey S, Alvarez X, et al. Monocyte/macrophage traffic in HIV and SIV encephalitis[J]. *J Leukoc Biol*, 2003, 74(5): 650–656.
- [19] Cenker JJ, Stultz RD, McDonald D. Brain microglial cells are highly susceptible to HIV-1 infection and spread[J]. *AIDS Res Hum Retroviruses*, 2017, 33(11): 1155–1165.
- [20] Miller MD, Warmerdam MT, Gaston I, et al. The human immunodeficiency virus-1 nef gene product: a positive factor for viral infection and replication in primary lymphocytes and macrophages[J]. *J Exp Med*, 1994, 179(1): 101–113.

- [21] Das SR, Jameel S. Biology of the HIV Nef protein[J]. *Indian J Med Res*, 2005, 121(4): 315–332.
- [22] Thompson KA, Kent SJ, Gahan ME, et al. Decreased neurotropism of *nef* long terminal repeat (*nef*/LTR)-deleted simian immunodeficiency virus[J]. *J Neurovirol*, 2003, 9(4): 442–451.
- [23] Fox HS, Gold LH, Henriksen SJ, et al. Simian immunodeficiency virus: a model for neuroAIDS[J]. *Neurobiol Dis*, 1997, 4(3-4): 265–274.
- [24] Patestas MA, Gartner LP. A textbook of neuroanatomy[M]. 2nd ed. Hoboken: John Wiley & Sons Inc., 2016.
- [25] Stein ME, Spencer D, Dansey R, et al. Biology of disease and clinical aspects of AIDS-associated lymphoma: a review[J]. *East Afr Med J*, 1994, 71(4): 219–222.
- [26] Omlin FX, Webster HD, Palkovits CG, et al. Immunocytochemical localization of basic protein in major dense line regions of central and peripheral myelin[J]. *J Cell Biol*, 1982, 95(1): 242–248.
- [27] Hirokawa N, Glicksman MA, Willard MB. Organization of mammalian neurofilament polypeptides within the neuronal cytoskeleton[J]. *J Cell Biol*, 1984, 98(4): 1523–1536.
- [28] Nath A. Pathobiology of human immunodeficiency virus dementia[J]. *Semin Neurol*, 1999, 19(2): 113–127.
- [29] Davis LE, Hjelle BL, Miller VE, et al. Early viral brain invasion in iatrogenic human immunodeficiency virus infection[J]. *Neurology*, 1992, 42(9): 1736–1739.
- [30] Buschmann JP, Berger K, Awad H, et al. Inflammatory response and chemokine expression in the white matter corpus callosum and gray matter cortex region during cuprizone-induced demyelination[J]. *J Mol Neurosci*, 2012, 48(1): 66–76.
- [31] Deshmane SL, Kremlev S, Amini S, et al. Monocyte chemoattractant protein-1 (MCP-1): an overview[J]. *J Interferon Cytokine Res*, 2009, 29(6): 313–326.
- [32] Prins M, Dutta R, Baselmans B, et al. Discrepancy in CCL2 and CCR2 expression in white versus grey matter hippocampal lesions of Multiple Sclerosis patients[J]. *Acta Neuropathol Commun*, 2014, 2: 98.
- [33] Grassi MP, Clerici F, Perin C, et al. Microglial nodular encephalitis and ventriculoencephalitis due to cytomegalovirus infection in patients with AIDS: two distinct clinical patterns[J]. *Clin Infect Dis*, 1998, 27(3): 504–508.
- [34] Alvarez-Carbonell D, Garcia-Mesa Y, Milne S, et al. Toll-like receptor 3 activation selectively reverses HIV latency in microglial cells[J]. *Retrovirology*, 2017, 14(1): 9.
- [35] Zhang JD, Liu JN, Katafiasz B, et al. HIV-1 gp120-induced axonal injury detected by accumulation of  $\beta$ -amyloid precursor protein in adult rat corpus callosum[J]. *J Neuroimmune Pharmacol*, 2011, 6(4): 650–657.
- [36] Jin JJ, Lam L, Sadic E, et al. HIV-1 Tat-induced microglial activation and neuronal damage is inhibited via CD45 modulation: a potential new treatment target for HAND[J]. *Am J Transl Res*, 2012, 4(3): 302–315.
- [37] Fu RY, Shen QY, Xu PF, et al. Phagocytosis of microglia in the central nervous system diseases[J]. *Mol Neurobiol*, 2014, 49(3): 1422–1434.
- [38] Toro P, Ceballos ME, Pesenti J, et al. Neurological soft signs as a marker of cognitive impairment severity in people living with HIV[J]. *Psychiatry Res*, 2018, 266: 138–142.

Submit to the *Journal* by ScholarOne Manuscripts at  
<http://mc03.manuscriptcentral.com/jbrint>

